

## ARTICLES

**Is There an Anionic Hofmeister Effect on Water Dynamics? Dielectric Spectroscopy of Aqueous Solutions of NaBr, NaI, NaNO<sub>3</sub>, NaClO<sub>4</sub>, and NaSCN****Wolfgang Wachter, Werner Kunz, and Richard Buchner\****Institut für Physikalische und Theoretische Chemie, Universität Regensburg, D-93040 Regensburg, Germany***Glenn Hefter\****Chemistry - DSE, Murdoch University, Murdoch, W.A. 6150, Australia**Received: June 20, 2005; In Final Form: July 20, 2005*

A systematic study of the dielectric relaxation spectra of aqueous solutions of NaBr, NaI, NaNO<sub>3</sub>, NaClO<sub>4</sub>, and NaSCN has been made over a wide range of frequencies ( $0.2 \leq \nu/\text{GHz} \leq 89$ ) and solute concentrations ( $0.05 \leq c/M \leq 1.5$ ) at 25 °C. The spectra could be adequately described by a single Cole–Cole (CC) process, symmetrically broadened relative to that of pure water. However, similar quality fits were also obtained with a three-Debye-process (3D) model consisting of a small ion-pair contribution at lower frequencies and two solvent relaxations at higher frequencies. Assuming the ions to be solvent separated, the 3D model provided estimates of their association constants and their rate constants for formation and dissociation. The bulk water relaxation times obtained from both models showed almost no dependence on the nature of the anion. Nevertheless, there were subtle differences in the concentration dependences of the relaxation times which correlated with some, but not all, of the anion properties that are believed to be relevant for explaining the anionic Hofmeister series.

**1. Introduction**

The Hofmeister series has been a scientific conundrum since its discovery in 1888. Originally observed from the effects of added electrolytes on protein solubilities,<sup>1,2</sup> Hofmeister sequences have been established for a great variety of chemical, biochemical, and biological phenomena.<sup>3–5</sup> A typical example is the effect of added salts on the salting in and salting out of argon or benzene by electrolytes in aqueous solutions. Such sequences, often referred to as specific ion effects or lyotropism, express themselves at relatively high concentrations (typically > 0.1 mol/kg) where short-range interactions start to dominate solution behavior. As Franks<sup>6</sup> and others<sup>3,7</sup> have pointed out, understanding of this series has barely moved beyond Hofmeister's original conjecture<sup>1</sup> that it was "probably related in some way to the affinities of different ions for water". Although there is a weak cation sequence, which appears to correlate well with hydration numbers,<sup>8</sup> Hofmeister effects are expressed most strongly among anions and these remain largely unexplained. The sequences may vary slightly with the substrate but are remarkably consistent. For protein solubilities they follow the general order:<sup>6</sup> (precipitate) SO<sub>4</sub><sup>2-</sup>, Cl<sup>-</sup>, Br<sup>-</sup>, I<sup>-</sup>, CNS<sup>-</sup>, ClO<sub>4</sub><sup>-</sup> (solubilize). Thus it seems that the key to understanding such series may lie in the interactions between anions and solvent water. Even though Hofmeister effects are essentially energetic,

they would be expected to influence the dynamic behavior of water, which is especially sensitive to changes in solute–solvent interactions.

Dielectric relaxation spectroscopy (DRS)<sup>9,10</sup> is a powerful technique for the study of ion–solvent interactions. DRS measures the response of a sample to an applied electromagnetic field, as a function of the field frequency,  $\nu$ . The complex permittivity  $\hat{\epsilon}(\nu) = \epsilon'(\nu) - i\epsilon''(\nu)$  so obtained can provide unique insights into the nature and dynamics of electrolyte solutions.<sup>7,11,12</sup> Surprisingly few DRS investigations of alkali metal salt solutions have been made<sup>13</sup> and most were performed only over limited ranges of concentration and/or frequencies. Inevitably, the data obtained were generally of much lower accuracy than is currently attainable.

Accordingly, a systematic investigation has been carried out on the dielectric spectra of the aqueous solutions of a series of sodium salts with a view to determining whether there is an anionic Hofmeister effect on water dynamics. The salts chosen — NaBr, NaNO<sub>3</sub>, NaI, NaSCN, and NaClO<sub>4</sub> — along with previous measurements,<sup>14–17</sup> cover the full range of the anionic Hofmeister series.<sup>6</sup>

**2. Experimental Section**

Solutions were prepared gravimetrically without buoyancy corrections; however, for data-processing purposes all concentrations are expressed in (mol solute)/(L solution), M. Densities required for the interconversion were obtained from the ELDAR database<sup>18</sup> for NaBr, NaI, NaNO<sub>3</sub>, and NaClO<sub>4</sub> or, for NaSCN,

\* To whom correspondence should be addressed: Richard.Buchner@chemie.uni-regensburg.de, g.hefter@murdoch.edu.au.

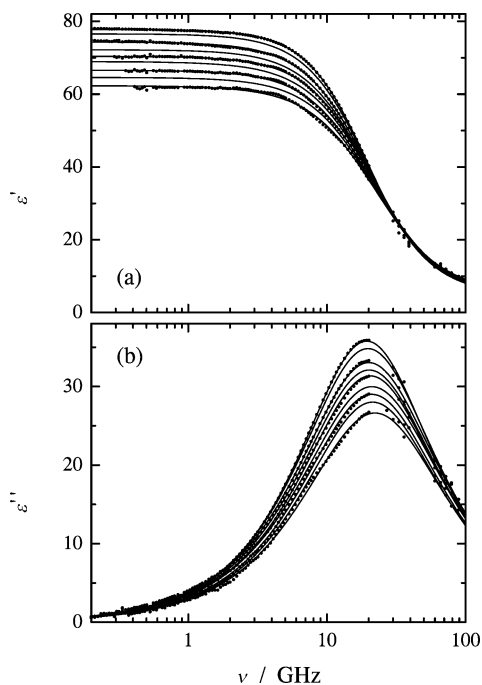


**Figure 1.** Dielectric permittivity (a) and loss (b) curves for NaBr(aq) at 25 °C and concentrations  $c/M = 0.05, 0.15, 0.35, 0.50, 0.65, 0.80, 1.00, 1.20,$  and  $1.40$  (top to bottom).

were determined using a vibrating-tube densimeter (Anton Paar DMA 60). All salts were commercial analytical reagents or better, dried under vacuum ( $\sim 1$  kPa) for at least 48 h at the following temperatures: NaBr (Fluka, BioChemica Ultra, >99.5% purity) at 80 °C, NaI (Merck, Suprapur, >99.5%) at 65 °C, NaNO<sub>3</sub> (Merck, Suprapur, >99.99%) at 100 °C, NaClO<sub>4</sub> (Merck, Pro analysi, >99%, recrystallized) at 160 °C, and NaSCN (Fluka, purum p.a., >99%) at 180 °C using P<sub>2</sub>O<sub>5</sub> (Sicapent, Merck) as a desiccant.

Dielectric spectra were recorded at  $\nu_{\min} \leq \nu/\text{GHz} \leq 20$  at Murdoch University using a Hewlett–Packard model 85070M Dielectric Probe System based on a HP 8720D Vector Network Analyzer (VNA), as described previously.<sup>14</sup> Temperature was controlled by a Hetofrig (Denmark) circulator-thermostat to  $\pm 0.02$  °C with an accuracy better than 0.1 °C. The value of the minimum frequency of investigation,  $\nu_{\min}$ , was determined by the conductivity contribution to the loss spectrum (see below). As such, it varied with concentration and salt type but was typically in the range of 0.2–0.5 GHz. All VNA spectra were recorded using at least two independent calibrations, with air, water, and mercury as the references. Higher frequency data for selected solutions were recorded at Regensburg using two interferometers: A-band ( $27 \leq \nu/\text{GHz} \leq 39$ ) and E-band ( $60 \leq \nu/\text{GHz} \leq 89$ ). The operation of these instruments is described in detail elsewhere.<sup>11,19</sup> Temperature control and accuracy were similar to those at Murdoch. Typical spectra and corresponding fits (see below) are shown in Figures 1 and 2; all fitting parameters are tabulated in the Supporting Information.

### 3. Data Analysis

For an electrolyte solution of conductivity  $\kappa$ , DRS determines the relative dielectric permittivity,  $\epsilon'(\nu)$ , and the total loss,  $\eta''(\nu)$ , which is related to the dielectric loss  $\epsilon''(\nu)$

$$\eta''(\nu) = \epsilon''(\nu) + \kappa/(2\pi\nu\epsilon_0) \quad (1)$$

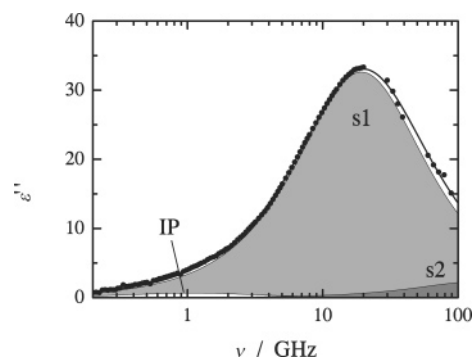


**Figure 2.** Dielectric loss curve of 0.35 M NaBr(aq) at 25 °C. Experimental data are described by a superposition of three Debye equations (3D model, eq 4); “IP” indicates the solute contribution arising from ion pairing, “s1” and “s2” are the contributions from the cooperative and the fast water relaxations, respectively.

where  $\epsilon_0$  is the permittivity of free space. To obtain  $\epsilon''(\nu)$  each VNA spectrum was analyzed separately to determine the slightly calibration-dependent effective conductivity at each concentration. As we did previously,<sup>15</sup>  $\kappa$  was obtained by fitting the experimental total loss curve to eq 1. The resulting  $\kappa$  values are generally 1–2% smaller than conventional (low-frequency) conductivity data<sup>18</sup> with slightly larger deviations at high electrolyte concentrations. Provided the  $\kappa$  values obtained in this way were sufficiently reproducible ( $\pm 2\%$  for at least two measurements) the averaged VNA spectra were combined with interferometer data. As can be seen from Figures 1 and 2 there is, in general, a seamless fit between the low- and high-frequency data although, as is usually observed for electrolyte solutions, the noise increases with increasing solute concentration (conductivity).<sup>14,15</sup>

The combined  $\hat{\epsilon}(\nu)$  data were analyzed by simultaneously fitting the in-phase ( $\epsilon'(\nu)$ , see Figure 1a) and out-of-phase ( $\epsilon''(\nu)$ , see Figure 1b) components to various relaxation models consisting of  $n$  distinguishable relaxation processes. Each process can be described by a Havriliak–Negami (HN) equation:<sup>20</sup>

$$\hat{\epsilon}(\nu) = \sum_{j=1}^n \frac{\epsilon_j - \epsilon_{j+1}}{[1 + (i 2\pi\nu\tau_j)^{1-\alpha_j}]^{\beta_j}} + \epsilon_\infty \quad (2)$$

where  $\epsilon_\infty$  ( $= \epsilon_{n+1}$ ) is the infinite-frequency permittivity,  $\tau_j$  is the average relaxation time for the  $j$ th dispersion step, and  $\alpha_j$  and  $\beta_j$  are empirical relaxation-time distribution parameters:  $0 \leq \alpha_j < 1$  and  $0 < \beta_j \leq 1$ . In principle  $\epsilon_\infty$  reflects only contributions from intramolecular polarizability; it can be obtained either from dielectric measurements at very high frequencies, or by the extrapolation of moderately high-frequency data, or as an additional fitting parameter in the analysis of  $\hat{\epsilon}(\nu)$  data (but see below). Note that  $S_j = \epsilon_j - \epsilon_{j+1}$  is the amplitude (relaxation strength) of the  $j$ th dispersion step and  $\epsilon = \epsilon_\infty + \sum S_j$  is the static (zero-frequency) permittivity of the sample.

Because of the importance of the major water relaxation and the rather subtle contributions from the other possible processes in the present solutions, it was found that satisfactory fits of the data could be obtained using either a Cole–Cole model ( $n = 1$ ;  $\beta_1 = 1$ ), or a three-Debye-process model ( $n = 3$ ;  $\alpha_j = 0$ ,  $\beta_j = 1$ ). Before discussing the relative merits of these models, it is crucial to briefly review existing knowledge of the dielectric spectrum for water because its relaxation processes dominate the dielectric spectra for all of the solutions investigated.

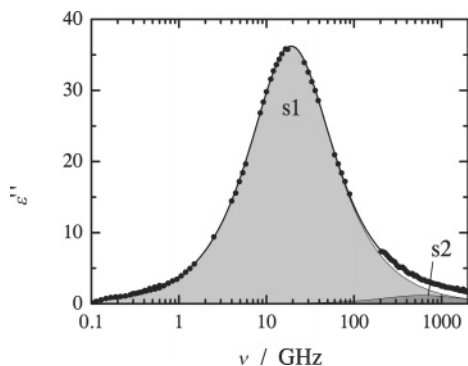


**Figure 3.** Dielectric loss curve of water at 25 °C. Experimental data are described by a superposition of two Debye equations (2D model) with “s1” and “s2” denoting the contributions of the cooperative and the fast water relaxations, respectively.

**3.1. Dielectric Spectrum of Water.** The dielectric spectrum for water at 25 °C over the range of frequencies of interest here is given in Figure 3; it is based on measurements in our laboratories and from other sources.<sup>13,21–23</sup> The observed spectrum is dominated by the process centered on 18 GHz ( $\tau_{s1} \approx 8$  ps), which is generally ascribed to the cooperative relaxation of bulk water molecules.<sup>21</sup> This process is the major contributor to all of the present solution spectra. Interpretation of the minor faster process, which is barely detectable at  $\nu < 100$  GHz in pure water and is sometimes shifted to higher frequencies in salt solutions, has long been controversial.<sup>21,23,24</sup> Recent studies,<sup>25</sup> combining data in the terahertz region ( $500 \leq \nu/\text{GHz} \leq 5000$ ) at varying temperatures with dielectric and far-IR spectroscopy, have shown that it is definitely a relaxation process centered on 600 GHz ( $\tau_{s2} \approx 0.25$  ps) rather than one of the low-energy intermolecular vibrations that occur at slightly higher frequencies.<sup>26</sup> Thus, the pure water spectrum over the frequency range investigated here,  $\nu \leq 89$  GHz, is best described as a combination of two Debye processes, with each  $\epsilon''(\nu)$  contribution having a Lorentzian shape.

**3.2. Dielectric Spectra of Aqueous Salt Solutions.** Despite the presence of two solvent relaxation processes, as just discussed, all of the investigated solutions could be reasonably fitted by a single Cole–Cole (CC) equation

$$\hat{\epsilon}(\nu) = \frac{\epsilon_{\text{CC}} - \epsilon_{\infty}}{1 + (i 2\pi\nu\tau_{\text{CC}})^{1-\alpha}} + \epsilon_{\infty} \quad (3)$$

where  $0 \leq \alpha < 1$  is a measure of the width of the distribution of relaxation times.<sup>9</sup> Note that the CC model describes a *symmetrically* broadened dielectric spectrum. The CC model yields an average relaxation time, here designated  $\tau_{\text{CC}}$  to avoid confusion, and the static permittivity of the solution,  $\epsilon$ , here labeled  $\epsilon_{\text{CC}}$ .

On the other hand, a superposition of three Debye equations (3D model)

$$\hat{\epsilon}(\nu) = \epsilon_{\infty} + \frac{\epsilon_{3\text{D}} - \epsilon_2}{1 + (i 2\pi\nu\tau_1)} + \frac{\epsilon_2 - \epsilon_3}{1 + (i 2\pi\nu\tau_2)} + \frac{\epsilon_3 - \epsilon_{\infty}}{1 + (i 2\pi\nu\tau_3)} \quad (4)$$

where  $\epsilon_{3\text{D}}$  is the static permittivity of the solution derived from the 3D model, generally yielded a better fit than the CC model even after allowance for the differing number of adjustable parameters. As discussed below, the lowest frequency process (of amplitude  $S_{\text{IP}} = \epsilon_{3\text{D}} - \epsilon_2$ ) in the 3D model is solute-related and is most plausibly ascribed to the presence of ion pairs (IP);

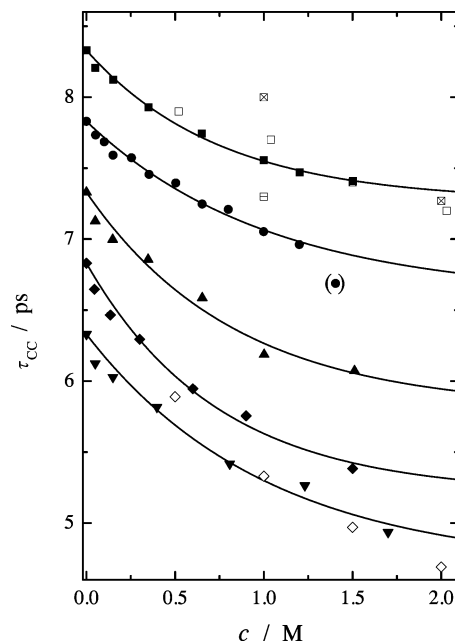


**Figure 4.** Concentration dependence of the relaxation times for aqueous solutions of sodium salts at 25 °C obtained with the Cole–Cole eq 3. Note that  $\tau_{\text{CC}}$  values have been shifted by varying amounts for representational clarity: NaNO<sub>3</sub> (black square), NaBr (black circle, −0.5 ps), NaI (black triangle, −1.0 ps), NaClO<sub>4</sub> (black diamond, −1.5 ps), and NaSCN (downwards black triangle, −2.0 ps). Also included are literature data for NaNO<sub>3</sub> (crosshatch square<sup>28</sup>; open square<sup>29</sup>; horizontal line square<sup>30</sup>), and NaClO<sub>4</sub> (open diamond<sup>31</sup>).

the two higher-frequency processes are the water relaxations discussed above.

However, it must be noted that, due to the small intensity of the low-frequency relaxation process for these electrolytes, it was not possible to generate a set of physically reasonable fitting parameters for all solutions using the 3D model. This effect, which is similar to that observed and discussed previously for CsCl(aq),<sup>27</sup> reflects a swamping of the weak ion-pair signal by the conductivity contribution. In this context it may be noteworthy that the  $S_{\text{IP}}/k$  ratio at which this effect becomes apparent is approximately constant for all systems of this type. The fitting parameters for the CC and 3D models are given in the Supporting Information, Tables 1 and 2.

Due to its symmetry, the CC model gives  $\tau_{\text{CC}}$  values comparable to the relaxation times  $\tau_2$  ( $\equiv \tau_{s1}$ ) derived from the 3D model. In contrast, a comparison between the static solution permittivities,  $\epsilon_{\text{CC}}$  and  $\epsilon_{3\text{D}}$ , and the solvent permittivity  $\epsilon_2$  given by the 3D model is less straightforward. Thus although  $\epsilon_{\text{CC}} \approx \epsilon_{3\text{D}}$ , their physical meaning is different, as discussed below.

## 4. Results and Discussion

**4.1. Relaxation Times from the Cole–Cole Model.** The relaxation times obtained by fitting the experimental spectra to the CC model, eq 3, decrease with increasing electrolyte concentration (Figure 4) for all of the present salt systems. Similar results were obtained previously for NaCl(aq),<sup>14</sup> KCl(aq), and CsCl(aq).<sup>27</sup> The variation in the relaxation times is well fitted by the exponential function

$$\tau(c) = a \exp(-bc) + (\tau(0) - a) \quad (5)$$

where the pure water value,  $\tau(0) = 8.33$  ps, was taken from Buchner et al.<sup>21</sup> Also included in Figure 4 are previously reported relaxation times for NaNO<sub>3</sub>(aq) and NaClO<sub>4</sub>(aq). The literature data for NaNO<sub>3</sub>(aq)<sup>28–30</sup> scatter around the present

**TABLE 1: Magnitude Parameter  $a$  and Sensitivity Parameter  $b$  from Eq 5 for the Present and Related Electrolytes<sup>a</sup>**

electrolyte	$a$	$b$
NaBr	$1.23 \pm 0.17$	$0.98 \pm 0.21$
NaI	$1.53 \pm 0.23$	$1.20 \pm 0.34$
NaNO <sub>3</sub>	$1.06 \pm 0.06$	$1.33 \pm 0.15$
NaClO <sub>4</sub>	$1.62 \pm 0.15$	$1.35 \pm 0.25$
NaSCN	$1.64 \pm 0.25$	$0.99 \pm 0.29$
NaCl	$1.60 \pm 0.12$	$0.79 \pm 0.12$
NaOH	$0 \pm 0.15$	0
Na <sub>2</sub> SO <sub>4</sub>	$1.55 \pm 0.09$	$1.8 \pm 0.2$
Na <sub>2</sub> CO <sub>3</sub>	$3.5 \pm 0.4$	$0.55 \pm 0.11$

<sup>a</sup> Units:  $a$  in ps;  $b$  in L mol<sup>-1</sup>.

values. In contrast, those of Barthel et al.<sup>28,31</sup> for NaClO<sub>4</sub>(aq) differ from the present results. However, it should be noted that their values were based on measurements at only five frequencies between 8 and 39 GHz, using less accurate equipment than that employed here.

The decrease of the relaxation times with increasing electrolyte concentration (Figure 4) corresponds to a weakening of the hydrogen-bond network,<sup>21</sup> which is typical for simple inorganic electrolytes in water. Both the relaxation times and their variation with  $c$  depend little on the nature of the anion (Figure 4, noting the offsets). This is quantified in the magnitudes of the empirical parameters  $a$  and  $b$  in eq 5, whose values are summarized in Table 1, along with those of related salts.<sup>16,17,27</sup>

The values of  $a$ , which reflect the high-concentration asymptote of the relaxation time (relative to pure water), are virtually identical for the present salt solutions, with the exception of Na<sub>2</sub>CO<sub>3</sub>(aq)<sup>17</sup> and to a much lesser extent NaNO<sub>3</sub>(aq). Chen et al.<sup>27</sup> found a linear correlation between the magnitude parameter  $a$  and the surface charge density  $\Phi$  ( $\propto r^{-2}$ ) of the cation for a limited number of simple salts in aqueous solution. However, as is apparent from the data in Table 1, no such correlation exists with respect to anions.

On the other hand, the  $b$  values, which represent the sensitivity of the relaxation time to concentration (the degree of curvature of the  $\tau_{CC}(c)$  plots), correlate moderately well with the anion radius  $r$  (Figure 5), with a correlation coefficient of  $R^2 = 0.88$  for an assumed linear fit. Radii (Table 2) were taken from Marcus<sup>32</sup> but note that, for NO<sub>3</sub><sup>-</sup>, the equatorial radius of  $206 \pm 7$  pm, rather than the axial radius of 126 pm, was adopted to account for the pronounced anisotropic hydration of this ion.<sup>40</sup> The older values of  $r(\text{SO}_4^{2-}) = 258$  pm<sup>41</sup> and  $r(\text{SCN}^-) = 199$  pm<sup>42</sup> are also included in Figure 5 for comparison as they align more closely with the correlation.

Although the Hofmeister series remains largely unexplained, recent theoretical work has suggested that dispersion forces may play an important role, particularly for anions.<sup>43</sup> Some correlation might therefore be expected between anion polarizability and water dynamics. Clearly, no significant correlation can exist with the essentially constant values of  $a$ , and a plot of  $b$  against anion polarizability, Figure 6, reveals only a weak, if any, correlation ( $R^2 = 0.4$  for a presumed linear fit). Note that polarizabilities (Table 2) were taken from Pyper et al.<sup>33</sup> except for SCN<sup>-</sup>, which was calculated from the molar refraction data given by Marcus.<sup>32</sup>

Another factor that may be important in explaining Hofmeister phenomena is the structure making/breaking characteristics of the ions. As noted above, the decrease in the water relaxation time with increasing electrolyte concentration (Figure 4) points to a weakening of the water structure arising from the added

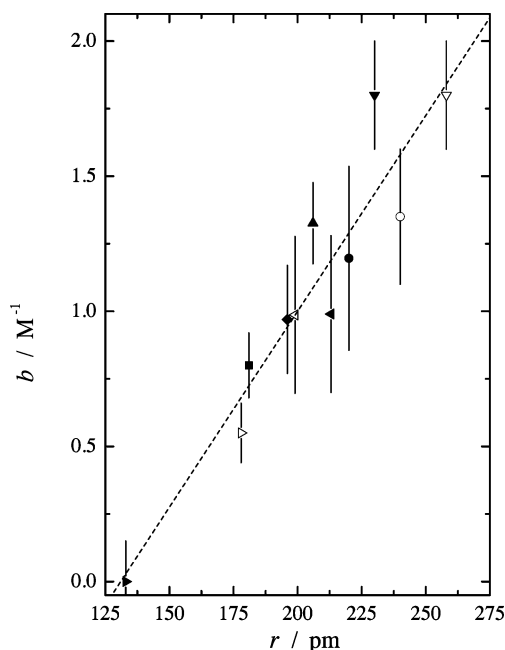


**Figure 5.** Sensitivity parameter,  $b$ , from eq 5 as a function of anion radius,<sup>32</sup>  $r$ : OH<sup>-</sup> (right pointing triangle), Cl<sup>-</sup> (black square), Br<sup>-</sup> (black diamond), I<sup>-</sup> (black circle), ClO<sub>4</sub><sup>-</sup> (○), NO<sub>3</sub><sup>-</sup> (upwards black triangle), SCN<sup>-</sup> (left pointing black triangle), SO<sub>4</sub><sup>2-</sup> (downwards black triangle), CO<sub>3</sub><sup>2-</sup> (right pointing open triangle). Also included are  $r(\text{SCN}^-)$  (left pointing open triangle) from Jenkins<sup>42</sup> and  $r(\text{SO}_4^{2-})$  (downwards open triangle) from Barthel et al.<sup>41</sup>

**TABLE 2: Anion Radius  $r$ ,<sup>32</sup> Polarizability  $\alpha$ ,<sup>33</sup> Coefficient of the Proton Relaxation Rate  $B_{\text{NMR}}$ ,<sup>34</sup> Viscosity Coefficient  $B$ ,<sup>35</sup> Wave Number of the OH Stretching Vibration  $\nu_1(\text{H}_2\text{O})$ ,<sup>36</sup> and the Stretching and Bending Vibrations<sup>37</sup> of Anion–Water Hydrogen Bonds in Aqueous Solution  $\nu_{\text{OH}\dots\text{X}}$  and  $\delta_{\text{OH}\dots\text{X}}$  Respectively<sup>a</sup>**

anion	$r$	$\alpha$	$B_{\text{NMR}}$	$B$	$\nu_1(\text{H}_2\text{O})$	$\nu_{\text{OH}\dots\text{X}}$	$\delta_{\text{OH}\dots\text{X}}$
OH <sup>-</sup>	133	2.3					
Cl <sup>-</sup>	181	3.76	-0.01	-0.005		$200 \pm 5$	$56 \pm 3$
Br <sup>-</sup>	196	5.08	-0.04	-0.033	3372	$182 \pm 5$	$42 \pm 3$
I <sup>-</sup>	220	7.41	-0.08	-0.073		$165 \pm 5$	$33 \pm 3$
ClO <sub>4</sub> <sup>-</sup>	240	5.45	-0.085	-0.058	3534		
NO <sub>3</sub> <sup>-</sup>	206	4.47	-0.05	-0.043	3420		
SCN <sup>-</sup>	213, 199 <sup>b</sup>	6.7 <sup>c</sup>	-0.07	0.022			
SO <sub>4</sub> <sup>2-</sup>	230, 258 <sup>d</sup>	$6.3 \pm 0.4$	0.12	0.206			
CO <sub>3</sub> <sup>2-</sup>	178	$5.4 \pm 0.4$	0.25	0.294	3350		

<sup>a</sup> Units:  $r$  in pm,  $\alpha$  in Å<sup>3</sup>,  $B_{\text{NMR}}$  in kg mol<sup>-1</sup>,  $B$  in L mol<sup>-1</sup>,  $\nu_1(\text{H}_2\text{O})$ ,  $\nu_{\text{OH}\dots\text{X}}$  and  $\delta_{\text{OH}\dots\text{X}}$  in cm<sup>-1</sup>. <sup>b</sup> From refs. 38,39. <sup>c</sup> From ref. 32. <sup>d</sup> From ref. 42.

ions. The notion of solvent structure making and breaking by ions is widely accepted in the literature and is supported by evidence from a variety of measurements including entropies, heat capacities, and viscosities.<sup>44</sup> Although there is no generally accepted quantitative measure of this effect, according to the various scales discussed by Marcus, all of the *present* salts contain structure breaking anions.<sup>32</sup> Figure 7 shows, with the definite exception of SO<sub>4</sub><sup>2-</sup> but including the structure making CO<sub>3</sub><sup>2-</sup>, that there is a reasonable inverse correlation for the present salts between  $b$  and the Jones–Dole viscosity  $B$  parameters (Table 2), which are often used as a measure of structure making/breaking.<sup>32</sup> There are similar correlations between  $b$  and other structure making/breaking parameters. These include (Table 2) the NMR water–proton relaxation time sensitivity parameter  $B_{\text{NMR}}$ <sup>32,34</sup> (not shown),<sup>45</sup> and the limited values for the symmetric IR vibration frequency,  $\nu_1(\text{H}_2\text{O})$  (Figure 8).<sup>36</sup> Inverse correlations (not shown) are also obtained

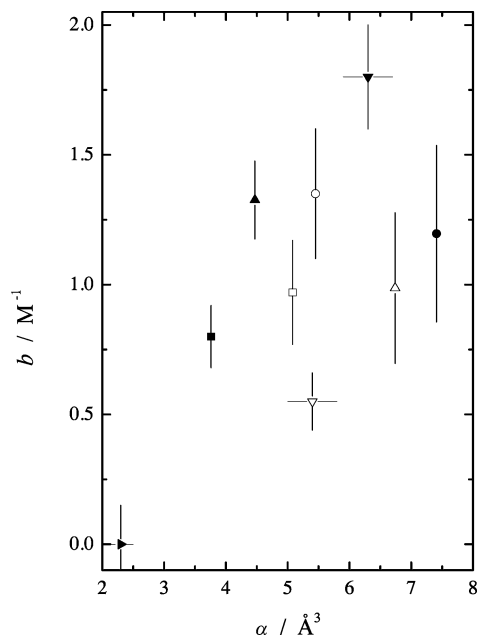


**Figure 6.** Sensitivity parameter,  $b$ , from eq 5 as a function of anion polarizability,  $\alpha$ :  $\text{OH}^-$  (right pointing black triangle),  $\text{Cl}^-$  (black square),  $\text{Br}^-$  (open square),  $\text{I}^-$  (black circle),  $\text{ClO}_4^-$  (open circle),  $\text{NO}_3^-$  (upwards black triangle),  $\text{SCN}^-$  (upwards open triangle),  $\text{SO}_4^{2-}$  (downwards black triangle),  $\text{CO}_3^{2-}$  (downwards open triangle).

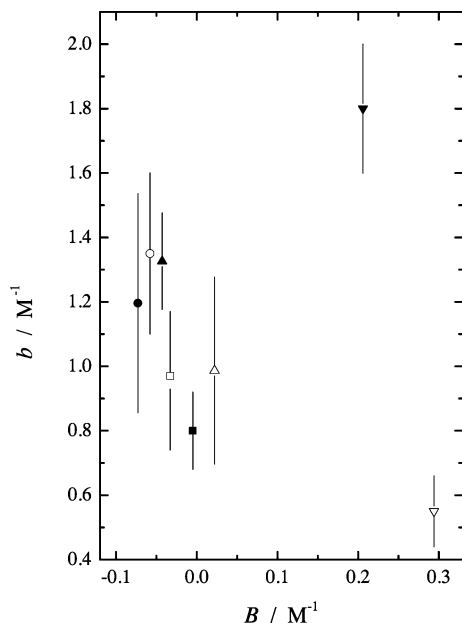


**Figure 7.** Sensitivity parameter,  $b$ , from eq 5 as a function of the viscosity coefficient,  $B$ , of the anions:  $\text{Cl}^-$  (black square),  $\text{Br}^-$  (open square),  $\text{I}^-$  (black circle),  $\text{ClO}_4^-$  (open circle),  $\text{NO}_3^-$  (upwards black triangle),  $\text{SCN}^-$  (upwards open triangle),  $\text{SO}_4^{2-}$  (downwards black triangle),  $\text{CO}_3^{2-}$  (downwards open triangle).

with the even more limited data available<sup>45</sup> (Table 2) for the stretching and deformation Raman bands for  $\text{O}-\text{H}\cdots\text{X}^-$  that occur at  $\sim 50$  and  $\sim 175$   $\text{cm}^{-1}$ .<sup>37</sup> However with regard to all of these correlations, it must be noted that the differences among the  $b$  values are small, the correlations are not especially strong, and there is usually one ion which does not fit the trend. It is particularly interesting that there is little correlation between the DRS results for anions and viscosities because such a correlation has been found between colligative properties of

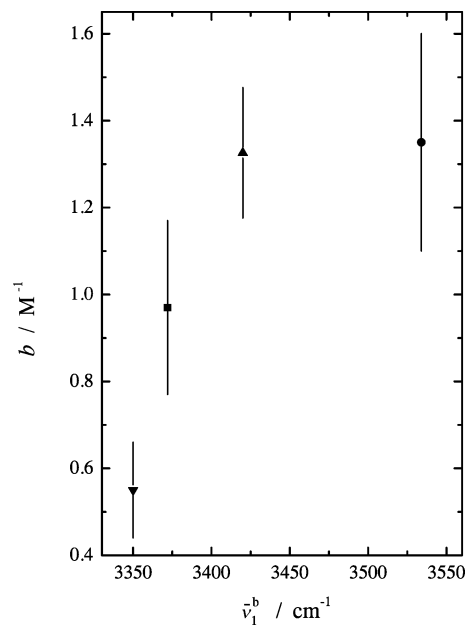


**Figure 8.** Sensitivity parameter,  $b$ , from eq 5 as a function of the position of the symmetric OH stretching vibration,  $\nu_1(\text{H}_2\text{O})$ , for different anions:  $\text{Br}^-$  (black square),  $\text{ClO}_4^-$  (black circle),  $\text{NO}_3^-$  (upwards black triangle),  $\text{CO}_3^{2-}$  (downwards black triangle).

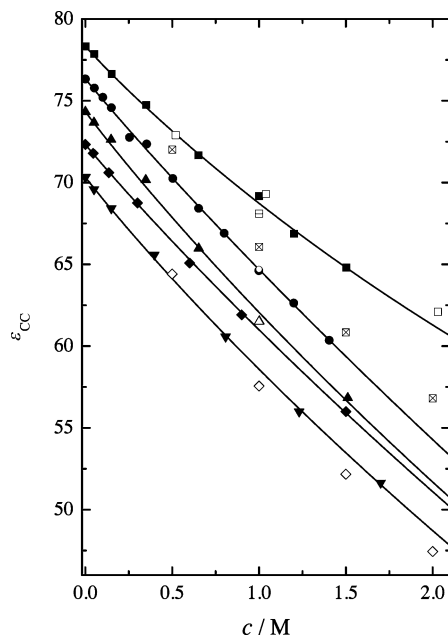


**Figure 9.** Static dielectric constant,  $\epsilon_{\text{CC}}$ , obtained from Cole–Cole fits as a function of electrolyte concentration,  $c$ . Note that  $\epsilon$  values have been shifted for representational clarity:  $\text{NaNO}_3$  (black square),  $\text{NaBr}$  (black circle,  $-2$ ),  $\text{NaI}$  (upwards black triangle,  $-4$ ),  $\text{NaClO}_4$  (black diamond,  $-6$ ), and  $\text{NaSCN}$  (downwards black triangle,  $-8$ ) solutions. Literature data:  $\text{NaNO}_3$  (crosshatched square<sup>28</sup>; open square<sup>29</sup>; horizontal line square<sup>30</sup>),  $\text{NaClO}_4$  (open diamond<sup>31</sup>),  $\text{NaBr}$  (open circle<sup>46</sup>), and  $\text{NaI}$  (upwards open triangle<sup>46</sup>).

cations and viscosities.<sup>8</sup> This again highlights the differences between cations and anions with respect to Hofmeister effects.

**4.2. Permittivities and Hydration Numbers from the Cole–Cole Model.** The static permittivity of each solution,  $\epsilon_{\text{CC}}$ , is derived directly by fitting the experimental data to the CC model. For all five electrolytes investigated in this work, the values of  $\epsilon_{\text{CC}}(c)$  (Figure 9, noting that offsets have been used for representational clarity) are remarkably similar but not

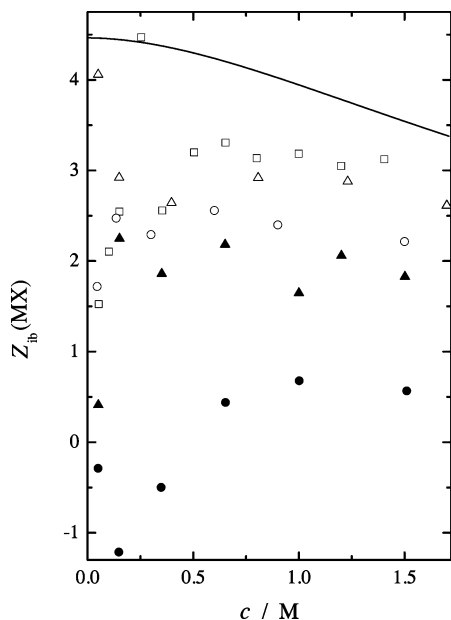


**Figure 10.** Number of irrotationally bound water molecules per mole of electrolyte,  $Z_{ib}(MX)$ , as a function of electrolyte concentration,  $c$ : NaBr (open square), NaI (black circle),  $\text{NaClO}_4$  (open circle),  $\text{NaNO}_3$  (black triangle) and NaSCN (upwards open triangle). The solid line is  $Z_{ib}(\text{Na}^+) = Z_{ib}(\text{NaCl})$  calculated from ref 14.

identical. They are well described as a function of concentration using the empirical equation

$$\epsilon = 78.33 + a_1c + a_2c^{1.5} \quad (6)$$

Figure 9 also includes literature data for the present systems, where available. The values of Giese et al.<sup>46</sup> for NaBr and NaI at  $c = 1$  M and the  $\text{NaNO}_3$  data of Filimonova et al.<sup>29</sup> and Kaatze<sup>30</sup> are in excellent agreement with the present results. In contrast, the values of Barthel et al. differ significantly for both  $\text{NaNO}_3$ <sup>28</sup> and  $\text{NaClO}_4$ <sup>31</sup> solutions. This is probably a reflection of the limited range of frequencies employed and their use of a single Debye equation to describe their data.

As described in detail elsewhere,<sup>14,16</sup> the dispersion amplitude of the solvent relaxation,  $S_s (= \epsilon_{CC} - \epsilon_\infty$  for the CC model), can be used to determine the apparent solvent concentration (the number of rotationally “free” solvent molecules),  $c_s^{\text{app}}$ , via the solvent-normalized Cavell equation<sup>47,48</sup>

$$c_s^{\text{app}} = \frac{2\epsilon(c) + 1}{2\epsilon(0) + 1} \frac{\epsilon(0)}{\epsilon(c)} \frac{(1 - \alpha_s f_s(c))^2 c_s^\alpha(0)}{(1 - \alpha_s f_s(0))^2 S_s(0)} S_s(c) \quad (7)$$

where  $\alpha_s$  is the polarizability and  $f_s$  the reaction field factor of water. The effective solvation number of the solute (the number of irrotationally bound solvent molecules),  $Z_{ib}$ , is then obtained by

$$Z_{ib} = (c_s^\circ - c_s^{\text{app}})/c \quad (8)$$

where  $c_s^\circ$  is the analytical concentration of the solvent.

This procedure, corrected for the kinetic depolarization of the ions assuming slip boundary conditions, has been shown to yield self-consistent  $Z_{ib}$  values for a variety of ions which are broadly comparable with effective hydration numbers from other techniques.<sup>14,15</sup> The  $Z_{ib}$  values so obtained for the present salts are plotted in Figure 10. Note that for these calculations  $\epsilon_\infty$  was fixed at 3.40, as reported for pure water by Hölzl et al.<sup>22</sup> from a thorough analysis of all the reliable high-frequency data

including far-infrared (THz) measurements. This value was adopted to reduce the scatter in the data that occurs by using the  $\epsilon_\infty$  values derived from the CC fits, although the  $Z_{ib}$  values obtained in that way (not shown) are similar to those shown in Figure 10.

As discussed elsewhere,<sup>14,15,49</sup> effective ionic solvation numbers,  $Z_{ib}(\text{ion})$ , can be obtained from the electrolyte values by making the reasonable assumption that chloride is unable to immobilize the surrounding water molecules, i.e.  $Z_{ib}(\text{Cl}^-) = 0$ . As the hydration of  $\text{Br}^-$ ,  $\text{I}^-$ , and  $\text{ClO}_4^-$  is expected to be even weaker than for  $\text{Cl}^-$ , the  $Z_{ib}$  values of these anions should be zero as well. Thus, for the aqueous solutions of NaBr, NaI, and  $\text{NaClO}_4$ ,  $Z_{ib}(\text{NaX})$  should be due only to  $\text{Na}^+(\text{aq})$ , and therefore, identical within experimental errors with  $Z_{ib}(\text{NaCl})$ . This is not the case. All  $Z_{ib}(\text{NaX})$  values obtained in this work (Figure 10) were significantly lower than  $Z_{ib}(\text{NaCl})$ .<sup>14</sup> For the most dilute NaI solutions, physically unreasonable negative  $Z_{ib}$  values were obtained.

From these observations, it might be postulated that  $Z_{ib}(\text{Cl}^-) \neq 0$  but instead, for instance,  $Z_{ib}(\text{I}^-) = 0$ . However, this would make  $Z_{ib}(\text{Na}^+) \approx 1$ , which is incompatible with the known strong interactions of this ion with water.<sup>50</sup> Also, the solvation numbers for  $\text{K}^+$  and  $\text{Cs}^+$  would then be negative,<sup>27</sup> and further inconsistencies would appear in other ionic hydration numbers obtained with DRS. An alternative interpretation of the present results might be that the stronger structure breakers (such as  $\text{I}^-$ ) disrupt the hydration of  $\text{Na}^+$  or perhaps just disturb the solvent structure sufficiently to give the appearance of negative  $Z_{ib}(\text{X}^-)$  values. Again, this is rather unlikely on the basis of scattering studies<sup>50</sup> and recent results from femtosecond pump-probe spectroscopy.<sup>51</sup> Yet another explanation of the observed effects might be the presence of generalized ion interactions (e.g. of the Pitzer type) such as  $\text{Na}^+/\text{X}^-$ ,  $\text{X}^-/\text{X}^-$ , and  $\text{X}^-/\text{Na}^+/\text{X}^-$  where the lifetime is too short to call them species. Such interactions would increase with increasing anion polarizability and therefore might account for the apparent decrease in  $Z_{ib}$ . The decreases of  $Z_{ib}$  at high concentrations of  $\text{NaCl}(\text{aq})$ <sup>14</sup> and  $\text{Na}_2\text{SO}_4(\text{aq})$ ,<sup>16</sup> for example, were indeed explained by increasing ion-ion interactions leading to a “melting” of the hydration shells. However, if this effect was operating with the observed magnitude at the low concentrations investigated here, then a strong anion-dependent decrease of  $Z_{ib}$  should also be seen. This is definitely not the case. If there is a concentration dependence at all, then it is in the opposite direction.

The only other plausible explanation for the anomalous values of  $Z_{ib}$  produced by the CC model is the possible presence of an additional low-frequency relaxation not due to water, but which is subsumed by the relaxation-time distribution parameter ( $\alpha > 0$ ) of the CC model. In this case  $\epsilon_{CC}$  would exceed the true static permittivity of the solvent and the water dispersion  $S_s(c)$  would be overestimated. This would, in turn, result in a too-small hydration number.

Thus it appears that despite the overall goodness of the data fit the CC model is not a fully appropriate description of the present dielectric spectra. Accordingly, consideration is now given to an alternative interpretation of the low-frequency part ( $< 5$  GHz) of  $\hat{\epsilon}(\nu)$ .

**4.3. Interpretation Using a 3D Model.** As already noted, the superposition of three Debye equations (the 3D model) provides a better fit of the present dielectric spectra than the CC model. The lowest-frequency process is consistent with an ion-pair relaxation while the two higher-frequency processes correspond closely to those observed for pure water (see section 3.1 and Figures 2 and 3).

However, application of the 3D model to the present spectra at higher salt concentrations produced unstable values of the relaxation time of the proposed low-frequency process,  $\tau_1$  (Supporting Information Table 2). For some salts, it became impossible to obtain physically reasonable fitting parameters using the 3D model. This effect almost certainly arises from the swamping of the small ion-pair contribution by the errors in the conductivity correction. A similar situation was observed previously for CsCl(aq)<sup>27</sup> at approximately the same value of  $S/\kappa$ . Also, even where fits are possible,  $\epsilon_2$  is rather noisy and so a direct analysis of the ion-pair amplitude,  $S_{IP} = \epsilon_{3D} - \epsilon_2$ , and the solvent dispersion,  $S_s = \epsilon_2 - \epsilon_\infty$ , is inappropriate. Thus no *direct* inferences regarding ion hydration and association are possible using the 3D model. However, as will be shown below, assumption of the existence of an ion-pair relaxation process combined with plausible estimates of  $Z_{ib}(X^-)$  allows a self-consistent and physically reasonable interpretation of the current DRS results.

With regard to the permittivities, if it is *assumed* that  $Z_{ib}(X^-) = 0$  for all of the present anions (and  $Cl^-$ ) then  $Z_{ib}(NaX) = Z_{ib}(NaCl) = Z_{ib}(Na^+)$ . As discussed above and elsewhere,<sup>14,15,49</sup> this assumption produces reasonable values for the effective solvation numbers of many ions. Using  $Z_{ib}(NaX)$  it is possible to estimate  $c_s^{app}$  and thus  $\epsilon_s(c)$ , the solvent permittivity in the solution, via eqs 7 and 8. As expected  $\epsilon_s(c)$  is smaller than the static permittivity of the solution,  $\epsilon$  ( $= \epsilon_{CC} \approx \epsilon_{3D}$ ), obtained from the experimental spectra. The difference between  $\epsilon(c)$  and  $\epsilon_s(c)$  can be attributed to a solute dispersion amplitude. Such values should be comparable to those obtained directly from the 3D model:  $S_{IP} = \epsilon_{3D} - \epsilon_2$ . This is indeed the case (Supporting Information Tables 1 and 2) for those (more dilute) solutions where the 3D model is applicable.

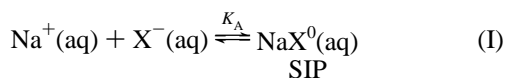
Proceeding along this path, ion-pair concentrations,  $c_{IP}$ , can be obtained using the Cavell equation, which for the present systems can be written

$$c_{IP} = \frac{3(\epsilon + (1 - \epsilon)A_{IP})k_B T \epsilon_0 (1 - \alpha_{IP} f_{IP})^2}{\epsilon N_A \mu_{IP}^2} (\epsilon - \epsilon_s) \quad (9)$$

where the subscript IP denotes an ion pair of dipole moment  $\mu_{IP}$  and polarizability  $\alpha_{IP}$ , with a reaction field factor  $f_{IP}$  and a shape factor  $A_{IP}$ , which can be calculated from the radii of the ions and of water as described previously.<sup>16</sup> Other symbols have their usual meanings<sup>52</sup> or have already been defined above.

To estimate the required ion-pair properties, an assumption must be made about the type and geometry of the ion pair.<sup>16</sup> Consistent with the well-established hydration shell of  $Na^+$  and the absence of significant irrotational binding of water by the present anions, only calculations based on solvent-shared ion pairs (SIPs) yielded physically meaningful results.

Values of the association constant,  $K_A$ , for the ion-pairing equilibrium



were therefore derived assuming only SIPs were formed. For convenience, these values were fitted to a Guggenheim-type equation<sup>53,54</sup>

$$\log K_A = \log K_A^o - \frac{2A_{DH}|z_+z_-|\sqrt{I}}{1 + A_K\sqrt{I}} + B_K I + C_K I^{3/2} \quad (10)$$

**TABLE 3: Empirical Parameters  $B_K$ ,  $C_K$ , and Association Constants,  $K_A^o$ , of Possible Ion Pairs for NaBr, NaI, NaClO<sub>4</sub>, NaNO<sub>3</sub>, and NaSCN in Aqueous Solution at 25 °C Obtained with Eq 10, Together with  $K_A^o$  Values from Conductivity Measurements<sup>a</sup>**

electrolyte	$B_K$	$C_K$	$K_A^o$	
			this work	literature
NaBr	$3.14 \pm 0.40$	$1.67 \pm 0.32$	$1.4 \pm 1.2$	$0.4^{57}, 0.8^{58}, 0.9^{59}$
NaI	$-0.24 \pm 0.30$	$-3.60 \pm 0.34$	$0.7 \pm 1.1$	$0.6^{56}$
NaClO <sub>4</sub>	$2.05 \pm 0.20$	$1.05 \pm 0.15$	$0.9 \pm 1.1$	$2.9^{60}$
NaNO <sub>3</sub>	$1.61 \pm 0.34$	$0.76 \pm 0.26$	$1.0 \pm 1.2$	$3.2^{61}$
NaSCN	$1.83 \pm 0.05$	$0.84 \pm 0.03$	$0.7 \pm 1.0$	

<sup>a</sup> Units:  $B_K$  in L mol<sup>-1</sup>,  $C_K$  in L<sup>3/2</sup> mol<sup>-3/2</sup>.

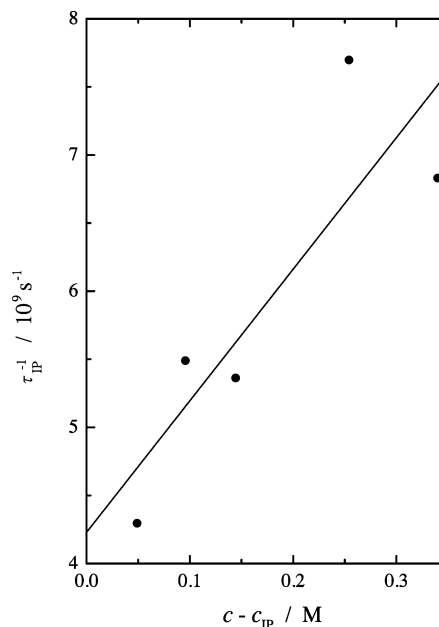


**Figure 11.** Ion pair relaxation rate,  $\tau_{IP}^{-1}$ , as a function of  $c - c_{IP}$  in aqueous NaBr solutions at 25 °C.

where the ionic strength  $I = c - c_{IP}$ ,  $K_A^o$  is the standard ( $I = 0$ ) value of  $K_A$ ,  $A_{DH}$  is the Debye–Hückel constant ( $0.5115 \text{ L}^{1/2}\text{mol}^{-1/2}$  for water at 25 °C),  $X_K$  are adjustable parameters ( $A_K$  was fixed at 1.00 throughout), and other symbols have their usual meanings.

The  $K_A^o$  values obtained in this way for the various salts are summarized in Table 3 along with the other fitting parameters for the Guggenheim equation. Also shown in Table 3 are literature estimates of  $K_A^o$ , based on high-precision conductivity measurements, which are generally in good agreement with the present results. It must be emphasized that better agreement cannot be expected because reliable determination of such small  $K_A^o$  values with any technique is problematic, not least because of the difficulties in separating the (very small) changes due to ion pairing and those associated with activity coefficient variation. These problems have been discussed at length elsewhere.<sup>55,56</sup> Assuming that the relaxation time of the slowest process in the 3D model can be attributed to ion pairs,  $\tau_1 = \tau_{IP}$ , knowledge of  $c_{IP}$  and  $K_A^o$  enables estimation of the rate constants for their formation,  $k_1$ , and decay,  $k_{-1}$ , via eq 11, where  $\tau_{or}$  is the rotational correlation time of the ion pair. These data yield<sup>62,63</sup>  $k_1$  from the slope of the linear regression of  $\tau_{IP}^{-1}$  vs  $I$  curve and  $k_{-1}$  from  $k_1/K_A^o$ .

$$\frac{1}{\tau_{IP}} = \frac{1}{\tau_{or}} + k_{-1} + 2k_1(c - c_{IP}) \quad (11)$$

As an example, a plot of  $\tau_{IP}^{-1}$  as a function of the free ion

**TABLE 4: Comparison of Experimental and Calculated<sup>a</sup> Rate Constants for the Formation,  $k_1$ , and Dissociation,  $k_{-1}$ , of Ion Pairs of NaBr, NaI, NaClO<sub>4</sub>, NaNO<sub>3</sub>, and NaSCN in Aqueous Solution at 25 °C<sup>b</sup>**

electrolyte	$k_1$	$k_1^D$	$k_{-1}$	$k_{-1}^D$
NaBr	4.8 ± 1.0	7.6	3.5 ± 2.3	9.9
NaI	3.0 ± 0.8	8.0	4.2 ± 5.4	9.2
NaClO <sub>4</sub>	7.8 ± 1.8	7.8	8.7 ± 8.8	7.8
NaNO <sub>3</sub>	1.7 ± 0.6	6.8	1.8 ± 1.5	9.4
NaSCN	8.0 ± 2.6	7.2	10 ± 11	8.1

<sup>a</sup> Via the Eigen theory, see eqs 12, 13. <sup>b</sup> Units  $k$ , in 10<sup>9</sup> L mol<sup>-1</sup> s<sup>-1</sup>,  $k_{-1}$  in 10<sup>9</sup> L mol<sup>-1</sup>.

concentration ( $c - c_{IP} = I$ ) is shown for NaBr in Figure 11. All the rate constants so obtained (Table 4) are of the order of magnitude expected with the Eigen theory<sup>64</sup> for diffusion-controlled processes (superscript D).

$$k_1^D = \frac{N_A z_+ z_- e_0^2}{\epsilon_0 \epsilon_s k_B T} \frac{D_+ + D_-}{\exp\left(\frac{z_+ z_- e_0^2}{4\pi\epsilon_0 \epsilon_s k_B T d}\right) - 1} \quad (12)$$

and

$$k_{-1}^D = \frac{3z_+ z_- e_0^2}{4\pi\epsilon_0 \epsilon_s k_B T d^3} \frac{D_+ + D_-}{1 - \exp\left(\frac{-z_+ z_- e_0^2}{4\pi\epsilon_0 \epsilon_s k_B T d}\right)} \quad (13)$$

where  $d$  is the cation–anion distance in the ion pair and all other symbols have their usual meanings.<sup>52</sup> The diffusivities (diffusion coefficients) of the ions,  $D_+$  and  $D_-$ , can be calculated from the single ion limiting conductivities,  $\lambda_i^\infty$ , by the Nernst–Einstein equation

$$D_i = \frac{RT}{|z_i| F^2 \lambda_i^\infty} \quad (14)$$

The ion-pair association constants and the rate constants for their formation and dissociation (Tables 3 and 4) are physically plausible. This suggests that, despite the difficulties in processing the data, it is reasonable to conclude that very small amounts of ion pairs do exist in most of these nominally strong electrolyte solutions.

As noted above it is extremely hard to produce definitive evidence for such weak ion pairs. This is especially true if the ion pairs are not contact species (CIPs) because the normally powerful spectroscopic methods (such as UV–vis, NMR, and Raman) cannot usually detect solvent-separated species.<sup>65,66</sup> Note too that conventional thermodynamic methods measure only the overall association and do not distinguish between the various ion pair types. Nevertheless, there are hints from such techniques that ion pairs exist in at least some of the present systems. Probably the strongest evidence comes from apparent molar volumes, which are unusually sensitive to ion pair formation.<sup>67,68</sup> This is because the charge neutralization “loosens” the hydration shells of the interacting ions, resulting in detectable positive deviations from the Debye–Hückel limiting law.<sup>67,69</sup> Even so, it is extremely difficult to perform such measurements with the requisite precision at sufficiently low concentrations to reliably quantify this effect. Bottomley et al.<sup>69</sup> have made suitably precise dilatometric measurements on aqueous solutions of various strong electrolytes down to unusually low concentrations. They found evidence for ion pairing in a number of them, putting

the strength of association in the order  $\text{ClO}_4^- < \text{NO}_3^- < \text{I}^- < \text{Br}^- < \text{Cl}^- < \text{OH}^- < \text{SO}_4^{2-}$ , albeit without presenting detailed evidence. The current results (Table 3) broadly agree with this order but are not sufficiently precise to allow more detailed discussion. All that can be said at the present time is that there is credible evidence for the formation of very small amounts of ion pairs in all of the present NaX(aq) systems.

On the other hand, the present results rule out the claim of Max and Chapados (ref 70 and references therein) based on measurements using attenuated total reflection infrared (ATR–IR) spectroscopy. These authors postulate that the observed water vibrations in concentrated salt solutions can be partitioned between pure (i.e. solvent) water and what the authors call “salt-saturated” water that is bound by the solute ions. They conclude<sup>70</sup> that “the clusters made up of 2 (with LiCl), 3 (with CsCl), 3.5 (with NaI), 4 (with KI or MgCl<sub>2</sub>), and 5 (with NaCl, KCl, NaBr, KBr, or CsI) molecules of water and one pair of salt ions are stable throughout the whole solubility range of these salts. These clusters behave as strongly bound units where the cation and anion in each cluster are inseparable.” If this statement, involving all ions in the solution, is correct, then, for example, an ion-pair dispersion amplitude of  $S_{IP} = \epsilon - \epsilon_s \approx 24$  would be expected for a 1 M solution of NaBr, if CIPs were the only species present ( $S_{IP} \approx 87$  for SIPs). Similar results can be calculated for the other salts. Such signals would be well above the detection limit of DRS and are totally inconsistent with observed  $S_{IP} \lesssim 3$  of this investigation. Also some of the hydration numbers of Max and Chapados, reported to be independent of concentration, are quite unbelievable. For example, they claim that MgCl<sub>2</sub> is *less* strongly solvated than NaCl, whereas virtually all physicochemical measurements<sup>67,71</sup> (including X ray and neutron diffraction,<sup>50</sup> activity coefficients, conductivities, and DRS<sup>72</sup> and other spectroscopic studies) and computer simulations<sup>73</sup> suggest the opposite. Many other anomalies are present in their hydration numbers, e.g. NaCl  $\approx$  KCl and NaBr  $\approx$  KBr, yet NaI < KI. It appears that the procedure of Max and Chapados does not produce realistic results.

#### 4.4. Is There a Hofmeister Effect on Water Dynamics?

The salts for this study were selected to span, in combination with previous data, the range of Hofmeister anions, from the protein-precipitating  $\text{SO}_4^{2-}$  to the solubilizing  $\text{ClO}_4^-$ . Although the interpretation of the present dielectric spectra has been complicated by the probable presence of a weak ion-pairing process at  $\sim 0.9$  GHz, the general pattern of behavior is clear: the impact of these anions (as their Na<sup>+</sup> salts) on water dynamics is remarkably similar. Thus, the nature of the anion appears to have almost no effect on the relaxation time of the bulk water network (Figure 4), even at the relatively high concentrations typically associated with Hofmeister effects. On the other hand, there *are* subtle differences in the concentration sensitivity of the solvent relaxation time, expressed in the  $b$  parameter in eq 5, at lower solute concentrations. The  $b$  values for the various salts correlate with their structure making/breaking character and (apparently) with their effect on H-bond strength. However, there is only a very weak correlation with anion polarizability, which is thought<sup>43</sup> to be important in producing Hofmeister effects.

The only reasonable conclusion at present is that while there may be an anionic Hofmeister effect on water dynamics, it is rather subtle. It appears more likely that Hofmeister effects reflect cooperative interactions between the anion, water, and a Hofmeister-sensitive solute, like a protein, or a macroscopic surface, without which such interactions are absent.



**Acknowledgment.** The authors thank Dr. Ting Chen for measuring the VNA spectra, and the Deutsche Forschungsgemeinschaft for a Mercator Visiting Professorship to G.H. and financial support to W.W.

**Supporting Information Available:** Tables showing conductivities and parameters of the CC and 3D models. This material is available free of charge via the Internet at <http://pubs.acs.org>.

## References and Notes

- Hofmeister, F. *Arch. Exp. Pathol. Pharmacol.* **1887**, 29, 1.
- Kunz, W.; Henle, J.; Ninham, B. W. *Curr. Opin. Colloid Interface Sci.* **2004**, 9, 19.
- Kunz, W.; Lo Nostro, P.; Ninham, B. W. *Curr. Opin. Colloid Interface Sci.* **2004**, 9, 1.
- Kim, H.-K.; Tuite, E.; Nordén, B.; Ninham, B. W. *Eur. Phys. J. E* **2001**, 4, 411.
- Collins, K. D.; Washabaugh, M. W. Q. *Rev. Biophys.* **1985**, 18, 323.
- Franks, F. *Water: A Matrix of Life*, 2nd ed.; R. Soc. Chem.: London, 2002.
- Barthel, J. M. G.; Krienke, H.; Kunz, W. *Physical Chemistry of Electrolyte Solutions*; Steinkopff/Springer: Darmstadt/New York, 1998.
- Zavitsas, A. A. *J. Phys. Chem. B* **2001**, 105, 7805.
- Böttcher, C. J. F.; Bordewijk, P. *Theory of Electric Polarization*, 2nd ed.; Elsevier: Amsterdam, 1978; Vol. 2.
- Scaife, B. K. P. *Principles of Dielectrics*; Clarendon: Oxford, 1989.
- Barthel, J.; Buchner, R.; Eberspächer, P.-N.; Münsterer, M.; Stauber, J.; Wurm, B. *J. Mol. Liq.* **1998**, 78, 83.
- Buchner, R.; Barthel, J. *Annu. Rep. Prog. Chem. C* **2001**, 97, 349.
- Barthel, J.; Buchner, R.; Münsterer, M. In *Electrolyte Data Collection, Part 2: Dielectric Properties of Water and Aqueous Electrolyte Solutions*; Kreysa, G. Ed., Chemistry Data Series; DECHEMA: Frankfurt am Main, 1995; Vol. 12.
- Buchner, R.; Hefter, G. T.; May, P. M. *J. Phys. Chem. A* **1999**, 103, 1.
- Buchner, R.; Hefter, G.; May, P. M.; Sipos, P. *J. Phys. Chem. B* **1999**, 103, 11186.
- Buchner, R.; Capewell, S. G.; Hefter, G.; May, P. M. *J. Phys. Chem. B* **1999**, 103, 1185.
- Capewell, S. G.; Buchner, R.; Hefter, G.; May, P. M. *Phys. Chem. Chem. Phys.* **1999**, 1, 1933.
- Barthel, J.; Popp, H. *J. Chem. Inf. Comput. Sci.* **1991**, 31, 107. Electrolyte Data Regensburg is a subset of the database DETHERM (distributor: STN, Karlsruhe, Germany).
- Barthel, J.; Bachhuber, K.; Buchner, R.; Hetzenauer, H.; Kleebauer, M. *Ber. Bunsen-Ges. Phys. Chem.* **1991**, 95, 853.
- Havriliak, S.; Negami, S. *J. Polym. Sci. C* **1966**, 14, 99.
- Buchner, R.; Barthel, J.; Stauber, J. *Chem. Phys. Lett.* **1999**, 306, 57.
- Hözl, C.; Schrödle, S.; Barthel, J.; Buchner, R., in preparation.
- Rønne, C.; Thrane, L.; Åstrand, P.-O.; Wallqvist, A.; Mikkelsen, K. V.; Keiding, S. R. *J. Chem. Phys.* **1997**, 107, 5319.
- Kaatze, U. *J. Solution Chem.* **1997**, 26, 1049.
- Sato, T.; Fukasawa, T.; Kunz, W.; Buchner, R., in preparation.
- Zelmann, H. R. *J. Mol. Struct.* **1995**, 350, 95.
- Chen, T.; Hefter, G.; Buchner, R. *J. Phys. Chem. A* **2003**, 107, 4025.
- Barthel, J.; Schmithals, F.; Behret, H. Z. *Phys. Chem. NF* **1970**, 71, 115.
- Filimonova, Z. A.; Lileev, A. S.; Lyashchenko, A. K. *Russ. J. Inorg. Chem.* **2002**, 47, 1890.
- Kaatze, U. *Ber. Bunsen-Ges. Phys. Chem.* **1973**, 77, 447.
- Barthel, J.; Krüger, J.; Schollmeyer, E. Z. *Phys. Chem. NF* **1977**, 104, 59.
- Marcus, Y. *Ion Properties*; Dekker: New York, 1997.
- Pyper, N. C.; Pike, C. G.; Edwards, P. P. *Mol. Phys.* **1992**, 76, 353.
- Hertz, H. G. In *Water – A Comprehensive Treatise*; Franks, F., Ed.; Plenum: New York London, 1973; Vol.3, Ch. 7.
- Jenkins, H. D. B.; Marcus, Y. *Chem. Rev.* **1995**, 95, 2695.
- Kleebauer, H.; Koçak, Ö.; Luck, W. A. P. In *Interactions of Water in Ionic and Nonionic Hydrates*, Kleebauer, H., Ed.; Springer: Berlin, 1987.
- Kanno, H.; Hiraishi, J. *J. Phys. Chem.* **1983**, 87, 3664.
- Marcus, Y. *Chem. Rev.* **1988**, 88, 1475.
- Marcus, Y. *J. Solution Chem.* **1983**, 12, 271.
- Krienke, H.; Schmeer, G. Z. *Phys. Chem.* **2004**, 218, 749.
- Barthel, J.; Gores, H. J.; Schmeer, G.; Wachter, R. *Top. Curr. Chem.* **1983**, 111, 33.
- Jenkins, H. D. B.; Thakur, K. P. *J. Chem. Educ.* **1979**, 56, 576.
- Ninham, B. W.; Yaminsky, V. *Langmuir* **1997**, 13, 2097.
- Marcus, Y. *J. Solution Chem.* **1994**, 23, 831.
- Wachter, W. Diploma Thesis, Universität Regensburg, Regensburg, Germany, 2004.
- Giese, K.; Kaatze, U.; Pottel, R. *J. Phys. Chem.* **1970**, 74, 3718.
- Cavell, E. A. S.; Knight, P. C.; Sheikh, M. A. *J. Chem. Soc., Faraday Trans.* **1971**, 67, 2225.
- Barthel, J.; Hetzenauer, H.; Buchner, R. *Ber. Bunsen-Ges. Phys. Chem.* **1992**, 96, 1424.
- Buchner, R.; Hözl, C.; Stauber, J.; Barthel, J. *Phys. Chem. Chem. Phys.* **2002**, 4, 2169.
- Ohtaki, H.; Radnai, T. *Chem. Rev.* **1993**, 93, 1157.
- Willem Omta, A.; Kropman, M. F.; Woutersen, S.; Bakker, H. J. *J. Chem. Phys.* **2003**, 119, 12457.
- Quantities, Units and Symbols in Physical Chemistry*, 2nd ed.; Mills, I.; Cvitaš, T.; Homann, K.; Kallay, N.; Kuchitsu, K., Eds.; Blackwell Scientific Publications: Oxford, 1993.
- Zemaitis, J. F., Jr.; Clark, D. M.; Rafal, M.; Scrivner, N. C. *Handbook of Aqueous Electrolyte Thermodynamics: Theory and Application*; American Institute of Chemical Engineers: New York, 1986.
- Robinson, R. A.; Stokes, R. H. *Electrolyte Solutions*, 2nd ed.; Butterworth: London, 1970.
- Duer, W. C.; Robinson, R. A.; Bates, R. G. *J. Chem. Soc., Faraday Trans. 1* **1972**, 68, 716.
- Pethybridge, A. D.; Spiers, D. J. *J. Chem. Soc., Faraday Trans. 1* **1977**, 73, 768.
- D'Aprano, A.; Capalbi, A.; Battistini, M. *J. Electroanal. Chem.* **1993**, 353, 121.
- Broadwater, T. L.; Kay, R. L. *J. Phys. Chem.* **1970**, 74, 3802.
- Esteso, M. A.; Grandoso, D. M.; Lemus, M. M. *J. Chem. Eng. Data* **1986**, 31, 215.
- Bury, R.; Justice, M. C.; Justice, J. C. *J. Chim. Phys. Phys. Chim. Biol.* **1970**, 67, 2045.
- Justice, M. C.; Bury, R.; Justice, J. C. *Electrochim. Acta* **1971**, 16, 687.
- Buchner, R.; Samani, F.; May, P. M.; Sturm, P.; Hefter, G. *ChemPhysChem* **2003**, 4, 373.
- Buchner, R.; Barthel, J. *J. Mol. Liq.* **1995**, 63, 55.
- Strehlow, H.; Knoche, W. *Fundamentals of Chemical Relaxation*; Verlag Chemie: Weinheim, 1977.
- Buchner, R.; Chen, T.; Hefter, G. *J. Phys. Chem. B* **2004**, 108, 2365.
- Rudolph, W. W.; Irmer, G.; Hefter, G. T. *Phys. Chem. Chem. Phys.* **2003**, 5, 5253.
- Marcus, Y. *Ion Solvation*; Wiley: Chichester, 1985.
- Marcus, Y.; Hefter, G. *Chem. Rev.* **2004**, 104, 3405.
- Bottomley, G. A.; Glossop, L. G.; Staunton, W. P. *Aust. J. Chem.* **1979**, 32, 699.
- Max, J.-J.; Chapados, C. *J. Chem. Phys.* **2001**, 115, 2664.
- Bockris, J. O'M.; Reddy, A. K. N. *Modern Electrochemistry I: Ionics*, 2nd ed.; Plenum: New York, 1998.
- Buchner, R. Dielectric Spectroscopy of Solutions, In *Novel Approaches to the Structure and Dynamics of Liquids: Experiments, Theories and Simulations*, Samios, J.; Durov, V. A., Eds.; NATO Science Ser. II; Kluwer: Dordrecht, 2004; Vol. 133.
- Rode, B. M.; Schwenk, C. F.; Randolph, B. R. Classical Versus Quantum Mechanical Simulations: The Accuracy of Computer Experiments in Solution Chemistry, In *Novel Approaches to the Structure and Dynamics of Liquids: Experiments, Theories and Simulations*; Samios, J., Durov, V. A., Eds.; NATO Science Ser. II, Kluwer: Dordrecht, 2004; Vol. 133.